Applied Surface Science xxx (2014) xxx–xxx

Contents lists available at ScienceDirect

Applied Surface Science

journal homepage: www.elsevier.com/locate/apsusc

Thermoelectric properties of $Bi_{0.5}Sb_{1.5}Te_3$ thin films grown by pulsed laser deposition

E. Symeou[a], M. Pervolaraki[a], C.N. Mihailescu[a,b], G.I. Athanasopoulos[a], Ch. Papageorgiou[a], Th. Kyratsi[a], J. Giapintzakis[a,*]

[a] Nanotechnology Research Center and Department of Mechanical and Manufacturing Engineering, University of Cyprus, 75 Kallipoleos Avenue, PO Box 20537, 1678 Nicosia, Cyprus
[b] National Institute for Laser, Plasma and Radiation Physics, 409 Atomistilor Street, PO Box MG-36, 077125 Magurele, Romania

ARTICLE INFO

Article history:
Received 4 July 2014
Received in revised form
19 September 2014
Accepted 9 October 2014
Available online xxx

Keywords:
Pulsed laser deposition
Bismuth-antimony telluride
Thermoelectric properties
Thin films

ABSTRACT

We report on the pulsed laser deposition of p-type $Bi_{0.5}Sb_{1.5}Te_3$ thin films onto fused silica substrates by ablation of dense targets of $Bi_{0.5}Sb_{1.5}Te_3$ with an excess of 1 wt% Te. We investigated the effect of film thickness, substrate temperature and post-annealing duration on the thermoelectric properties of the films. Our results show that the best power factor (2780 $\mu W/K^2m$ at 300 K) is obtained for films grown at room temperature and then post-annealed in vacuum at 300 °C for 16 h. This is among the highest power factor values reported for $Bi_{0.5}Sb_{1.5}Te_3$ films grown on fused silica substrates.

1. Introduction

Thermoelectric devices are of interest for applications as power generators and heat pumps, which interconvert heat and electricity via the Seebeck and the Peltier effect, respectively. The performance of these solid state thermoelectric energy converters depends on the dimensionless thermoelectric figure of merit (ZT) of the materials, given by $ZT = S^2T/\rho\kappa_t$, where S, ρ, κ_t, and T are the Seebeck coefficient, electrical resistivity, total thermal conductivity, and absolute temperature, respectively. A good thermoelectric material must combine a large Seebeck coefficient S with low electrical resistivity ρ and low thermal conductivity κ_t. Another crucial criterion to characterize thermoelectric materials is the power factor, defined as $PF = S^2/\rho$ [1].

Bulk $Bi_{0.5}Sb_{1.5}Te_3$ (BST) is considered as a state-of-the-art p-type thermoelectric material in the temperature range 273–473 K because it exhibits high power factor and low thermal conductivity over this temperature range. For example, Caillat et al. [2] have reported that single crystals of BST exhibit a power factor of 4800 $\mu W/K^2m$ and a thermal conductivity of 1.51 W/mK at 300 K. In addition, Kitagawa et al. [3] have recently reported that BST pellets fabricated by mechanical alloying and hot pressing exhibit a power factor of 3600 $\mu W/K^2m$ at 300 K.

The development of thermoelectric thin films has brought a new perspective to the integration of thermoelectric cooling devices into microelectronic systems for thermal management purposes. Several techniques have been employed to deposit BST thin films on a variety of substrates including flash evaporation [4], radio-frequency sputtering [5,6], direct current magnetron sputtering [7,8], and pulsed laser deposition (PLD) [9,10]. In these studies, it has been shown that the thermoelectric properties of BST films depend on several parameters including type of substrate, substrate temperature, film thickness and post-annealing treatment. Nevertheless, the deposition of BST thin films with bulk-like thermoelectric properties remains a challenge because of issues related to stoichiometry and antisite defects.

PLD is considered to be a good method to obtain stoichiometric transfer of material from target to a film on a substrate even in the case of a multicomponent compound [11]. As there are not many works on the growth of BST films by PLD, we have carried out a systematic investigation on this topic using targets with excess of Te to compensate for possible Te volatilization losses due to its high vapor pressure [12]. We used PLD to deposit BST thin films by laser ablating dense targets of $Bi_{0.5}Sb_{1.5}Te_3$ with an excess of 1 wt% Te. The films were deposited on fused silica substrates at various temperatures between room temperature and 350 °C. We

* Corresponding author. Tel.: +357 22892283.
E-mail address: giapintz@ucy.ac.cy (J. Giapintzakis).

http://dx.doi.org/10.1016/j.apsusc.2014.10.038
0169-4332/

investigated the effect of substrate temperature, film thickness and post-annealing duration on the thermoelectric properties of the films.

2. Experiment

2.1. Film deposition

A KrF* excimer laser (wavelength 248 nm, pulse width 25 ns) operating at 10 Hz was used to ablate home-made BST targets with excess of Te. The PLD targets (BST + 1 wt% Te) were made by mixing high purity metals of Bi, Sb and Te in the desired amounts and melting them at 850 °C in an evacuated sealed quartz tube. The obtained ingots were ground using an agate mortar and pestle. The resulting fine powder was cold pressed at 4 kbars into 15 mm diameter disks. The films were deposited on low thermal conductivity fused silica substrates. Prior to deposition the substrate was cleaned thoroughly in an ultrasonic bath and then was mounted in a vacuum chamber, opposite to the target at a distance of 4 cm. The chamber was evacuated to a base pressure of $\sim 4 \times 10^{-6}$ mbar prior introducing ~0.13 mbar of high purity Ar gas. The laser beam was incident on the target at 45° and the laser ablation fluence was 2 J/cm^2. The target was continuously rotated and rastered to avoid local heating of the target and achieve stoichiometric films. We deposited BST films at various substrate temperatures between room temperature and 350 °C in order to obtain the optimum growth conditions, which result in the best power factor (PF). Films with different thicknesses were produced in order to investigate the effect of thickness on PF. Also, BST films were grown at room temperature and then were subjected to a post-annealing process. Based on published reports, we selected to perform the annealing process at 300 °C in argon atmosphere and vacuum for different times: (Ar – 5 h, 10 h and 16 h; vacuum – 16 h) [7].

2.2. Film characterization

The structure, morphology and chemical stoichiometry of the BST thin films were characterized using techniques such as grazing incidence X-ray diffraction (GIXRD), scanning electron microscopy (SEM) and energy dispersive X-ray spectroscopy (EDX), respectively. EDX spectra were collected under the same conditions (accelerating voltage, beam current, magnification, and acquisition time) from at least three different regions of each sample. Quantitative analysis of the different elements (atomic percent concentration) was performed by standard-less analysis with 3% accuracy. The thickness of the films was measured using an optical profilometer.

The temperature dependence of electrical resistivity and Seebeck coefficient as well as the Hall coefficient at 300 K were measured using a commercial physical properties measurement system (PPMS, Quantum Design). The Seebeck coefficient was measured using the steady state technique with thermal gradients of 1% of the measurement temperature and miniature Cernox temperature sensors. The distance between the voltage leads and the temperature sensors was about 1 mm. The electrical resistivity was measured using the four-probe ac method. Electrical resistivity and Seebeck coefficient were measured simultaneously on samples with width of 5 mm and length of 10 mm using the Thermal Transport Option (TTO) of PPMS. A picture of a typical sample is shown in Fig. 1. The Hall coefficient was measured using the Van der Pauw under a magnetic field of 2 T. The total relative errors in the measurements of electrical resistivity, thermopower and carrier density are about 5%, 7% and 5%, respectively.

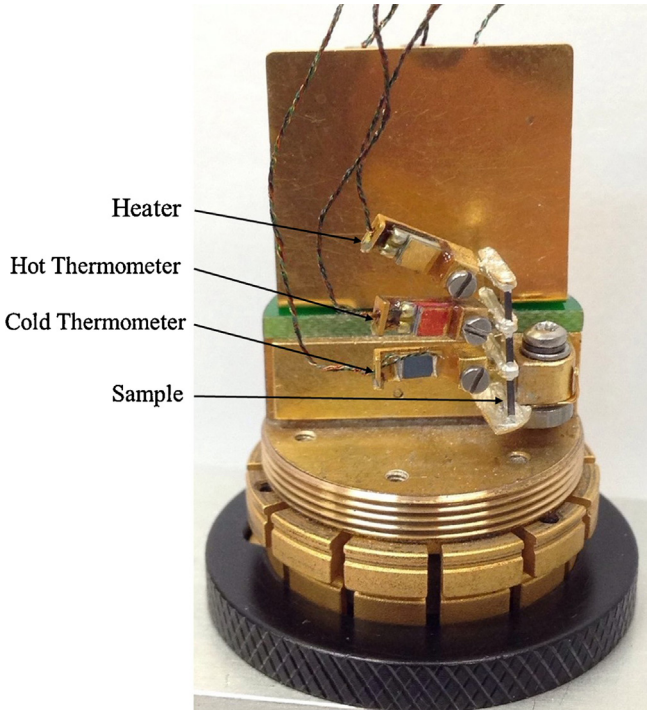

Fig. 1. Picture of a typical sample for resistivity and Seebeck coefficient measurements using the thermal transport option (TTO PPMS, Quantum Design).

3. Results and discussion

3.1. Effect of thin film thickness

In order to investigate the influence of film thickness on the thermoelectric properties of BST films, a series of samples were grown at 350 °C by varying the number of laser pulses and keeping the rest of the deposition conditions identical. The thickness of the as-grown films varied between 100 nm and 480 nm and was found to be a crucial parameter for their thermoelectric properties. All samples exhibit similar XRD patterns (not shown); i.e., they are all fully oriented and the observed (0 0 l) reflections indicate preferential growth along the *c*-axis.

Films thicker than 280 nm have microcracks and the coalescence of these cracks leads to exfoliation. This effect is attributed to the large difference in the thermal expansion coefficient between the fused silica substrate (1×10^{-6}/K) and the BST films ($\sim 20 \times 10^{-6}$/K). Specifically, the large thermal expansion coefficient mismatch generates cracks in the films due to the large tensile thermal strains induced upon cooling down to room temperature following the deposition of the films.

On the other hand, BST films thinner than 180 nm are dense with smooth surfaces. As shown in Table 1, the best power factor at 300 K is obtained for 180 nm-thick films, i.e., PF = 2150 μW/K^{2}m, because of its lower resistivity than the other samples. Given that all samples are fully oriented along *c*-axis, we expect the effect of anisotropy to be weak, and hence, we propose that the lower resistivity value of the 180 nm-thick sample is a thickness effect; i.e.,

Table 1
Room-temperature thermoelectric properties of BST films with different thicknesses.

Thickness (nm)	ρ (Ω m)	S (μV/K)	PF (μW/K^{2}m)
120	9.3×10^{-6}	128	1756
180	8×10^{-6}	135	2150
280	1×10^{-5}	120	1398

Please cite this article in press as: E. Symeou, et al., Thermoelectric properties of $Bi_{0.5}Sb_{1.5}Te_3$ thin films grown by pulsed laser deposition, Appl. Surf. Sci. (2014), http://dx.doi.org/10.1016/j.apsusc.2014.10.038

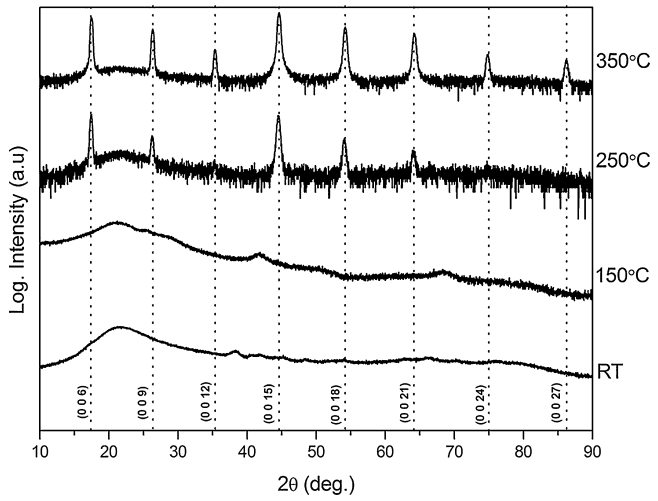

Fig. 2. Grazing incidence X-ray diffraction patterns for BST films deposited at different substrate temperatures.

the surface scattering of charge carriers is reduced resulting in the increase of the carrier mean free path [4]. The fact that all samples exhibit similar thermopower values indicates that the carrier concentration for all samples is also similar, and thus, the difference in resistivity should be related to differences in mobility as argued above.

3.2. Effect of substrate temperature

Fig. 2 shows the GIXRD patterns of BST thin films deposited at different substrate temperatures. It is evident that the films grown at substrate temperatures lower than 150 °C are amorphous and as the substrate temperature increases above 150 °C the crystallinity of the films improves. The increase of the substrate temperature to 350 °C is associated with the generation of new peaks in the GIXRD pattern. The film deposited at 350 °C is fully oriented and the observed (0 0 l) reflections indicate preferential growth along the *c*-axis of the BST film. SEM images (not shown) from the same series of BST thin films reveal that all films consist of platelet-like grains and the grain size increases slightly with increasing substrate temperature.

The stoichiometric transfer of material from target to film is a challenge in the case of the investigated compound as it is composed of three elements with different atomic weights and vaporization enthalpies [12]. The composition of the BST films was investigated by EDX. Table 2 shows the composition analysis of the films deposited at different substrate temperatures and of the BST target used for their deposition by PLD. The target seems to be nearly stoichiometric concerning the atomic ratio of (Bi + Sb):Te. It is known that EDX may not be the best method to determine accurately the atomic concentration of BST samples as the peaks corresponding to Sb and Te overlap and this makes difficult the analysis of the spectra [13]. However, we suggest that by concentrating on the Bi atomic concentration it is possible to extract useful information because the Bi peak is well defined and the associated error with the deduced at% concentration is rather small. It is evident from Table 2 that the Bi concentration tends to increase with increasing substrate temperature possibly due to the loss of Te. We expect therefore the concentration of Bi_{Te} antisite defects to increase with a corresponding increase in the carrier concentration. This expectation is confirmed by the measured room-temperature carrier concentration values shown in the last column of Table 2.

Table 2
EDX composition analysis for BST target used and films deposited at different temperatures. Room-temperature carrier concentrations for BST films deposited at 150, 250 and 350 °C.

Sample	Bi (at%)	Sb (at%)	Te (at%)	Carrier concentration at 300 K (cm^{-3})
Target (BST + 1 wt%)	10.73	28.83	60.24	–
Film – RT	8.78	29.31	61.91	–
Film –150 °C	10.40	29.00	60.60	2.54×10^{19}
Film –250 °C	9.38	28.84	61.78	1.09×10^{20}
Film –350 °C	11.65	28.18	60.17	1.44×10^{20}

The effect of the substrate temperature on the electrical resistivity of BST films is illustrated in Fig. 3a. The almost-amorphous film grown at 150 °C exhibits semiconducting-like behavior whereas the crystalline films grown at 250 °C and 350 °C exhibit metallic-like behavior. The transition from semiconducting to metallic behavior with increasing substrate temperature is attributed both (i) to the increase of the hole carrier concentration due to the increase of Bi_{Te} antisite defects (vide supra) and (ii) to the increase of the hole carrier mobility due to enhanced crystallinity and texturing of the films. The above reasons are the origin of the large difference in the resistivity of the samples exhibiting metallic behavior.

The effect of the substrate temperature on the Seebeck coefficient (S) of BST films is shown in Fig. 3b. It is evident that S tends to decrease with increasing substrate temperature. This effect is attributed to the fact that S is inversely proportional to the carrier concentration and also to the electronic anisotropy (out-of-plane S is greater that in-plane S) which is directly related with the texturing of the films. Fig. 3c displays the temperature dependence of the calculated power factor values for all films. The film deposited at 350 °C exhibits the best power factor over the entire temperature range investigated; e.g., at 300 K PF = 2278 $\mu W/K^2m$.

3.3. Effect of post annealing

Post-annealing treatment is usually applied to improve film stoichiometry, reduce point defects and finally, improve the thermoelectric properties of the films [6]. Fig. 4 shows the XRD patterns for a BST film which was deposited at room temperature and then post-annealed in Ar atmosphere at 300 °C for 16 h. The as-grown BST film exhibits amorphous structure (cf. lower panel of Fig. 4) while following post-annealing the same film becomes crystalline with randomly oriented grains (cf. upper panel of Fig. 4). It is noted that a polycrystalline structure was observed for all post-annealed BST films. Thus, the annealing process enhances the crystallinity of the films but does not result in preferred orientation.

SEM imaging (not shown) reveals that annealing in Ar atmosphere results in the formation of particles (i.e., film surface becomes rougher) and their areal density increases with increasing annealing duration. On the other hand, films annealed in vacuum have significantly less and smaller in size particles on their surface than the ones annealed in Ar atmosphere. The particles for both types of annealing were found to have the same composition as the bulk of the film. A similar effect has also been reported by Bourgault et al. [14] and it needs further investigation.

The results of the composition analysis for the BST films, deposited at room temperature and then post-annealed in Ar atmosphere and vacuum, are illustrated in Table 3. The as-deposited films seem to be rich in Bi with the exception of the film that was post-annealed in vacuum. Following the post-annealing treatment, all films display an increase in Bi concentration, which is attributed to loss of the highly volatile Te during the annealing process. We expect therefore all post-annealed films to exhibit p-type conduction as acceptor-like Bi_{Te} antisite defects are likely to be formed due to excess of Bi ions [14,15]. In addition, we expect the resistivity of the films to decrease with increasing annealing duration because

Please cite this article in press as: E. Symeou, et al., Thermoelectric properties of $Bi_{0.5}Sb_{1.5}Te_3$ thin films grown by pulsed laser deposition, Appl. Surf. Sci. (2014), http://dx.doi.org/10.1016/j.apsusc.2014.10.038

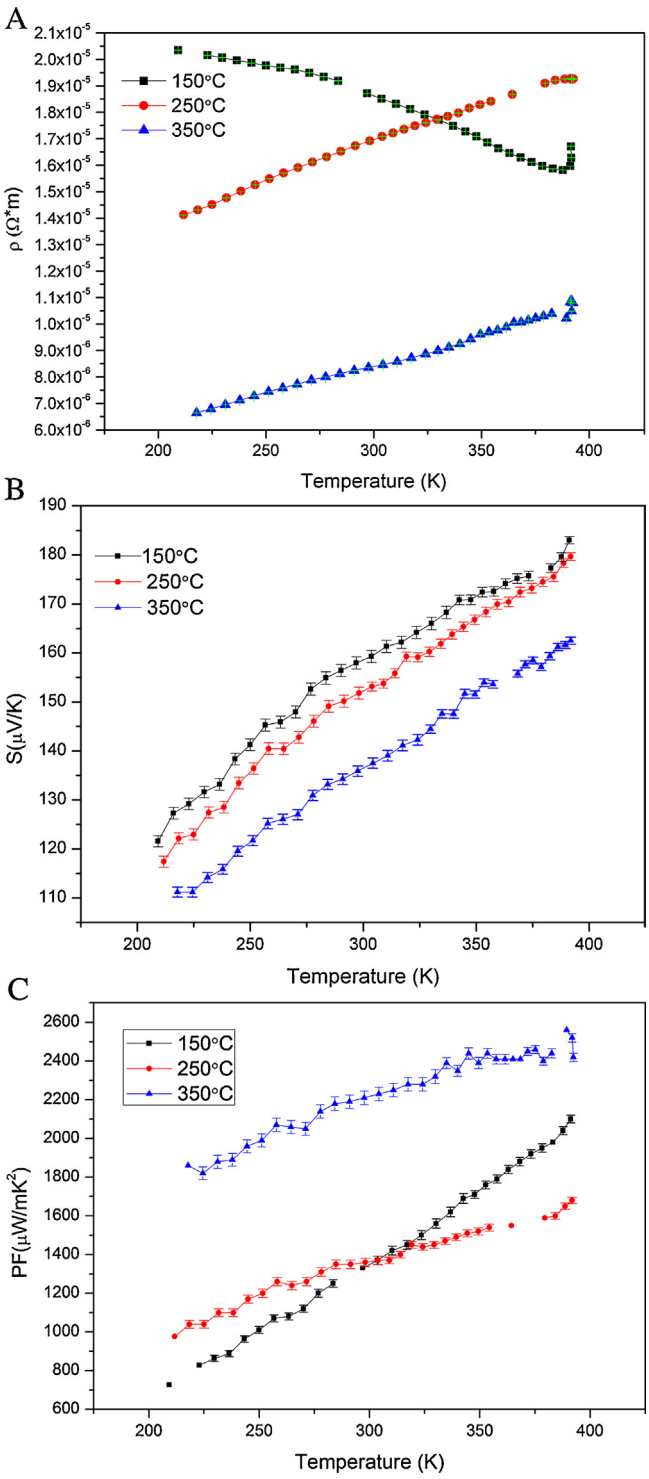

Fig. 3. Temperature dependence of electrical and thermoelectric properties of BST films grown at different substrate temperatures: (a) electrical resistivity, (b) Seebeck coefficient, and (c) power factor.

the concentration of the Bi_{Te} antisite defects is likely to increase resulting in an increase of the hole carrier concentration.

As can be seen in Fig. 5, the thermoelectric properties of the films are strongly influenced by the post-annealing treatment. Fig. 5a displays the temperature dependence of the Seebeck coefficient for BST films annealed at 300 °C for different duration times of 5, 10 and 16 h. Interestingly while the magnitude of the Seebeck coefficient remains almost the same (~210–220 μV/K at 300 K)

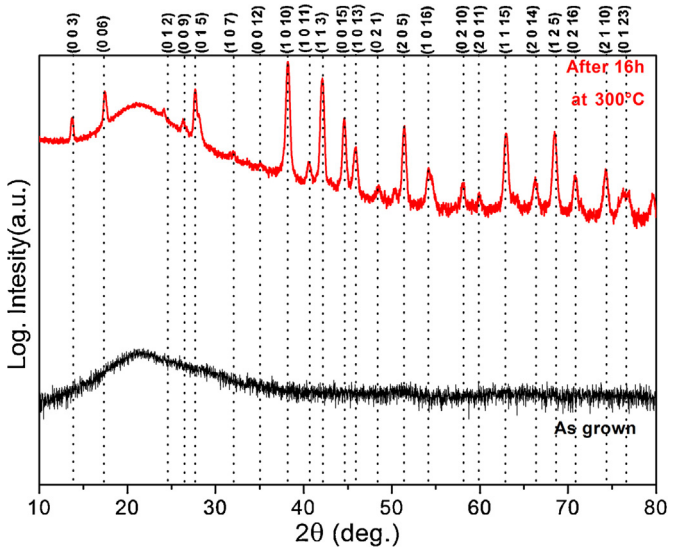

Fig. 4. Grazing incidence X-ray diffraction pattern obtained for a BST film deposited at room temperature and then post-annealed in Ar atmosphere at 300 °C for 16 h.

for all films annealed in Ar atmosphere there is a definite trend in the S magnitude which is consistent with the trend of the hole carrier concentrations (p) (cf. last column of Table 3); i.e., $S(10\,h) > S(5\,h) > S(16\,h)$ whereas $p(10) < p(5\,h) < p(16\,h)$. This indicates that the S value is strongly dependent on the concentration of the antisite defects and the stoichiometry of the films. On the other hand, the resistivity, which shows metallic behavior in agreement with [14], exhibits a different trend, i.e., $\rho(5\,h) > \rho(10\,h) > \rho(16\,h)$ (Fig. 5b). This effect may be attributed to the fact that the grain size increases with increasing annealing duration, i.e., the density of the grain boundaries decreases, and thus, the hole carrier mobility is enhanced [6]. The resistivity being affected by both parameters, carrier concentration and carrier mobility, tends to then have the observed trend.

In comparison with the films post-annealed in Ar, the Seebeck coefficient of the film post-annealed in vacuum decreases to slightly lower values (190 μV/K at 300 K) and its resistivity drops significantly about a factor of 2. As a result the BST film, which was annealed in vacuum, exhibits the best power factor among all the films discussed herein and is equal to 2780 $\mu W/K^2m$ at 300 K and 3200 $\mu W/K^2m$ at 390 K (cf. Fig. 5c). These PF values are among the highest ones reported for BST films grown on fused silica substrates. The origin of the power factor enhancement in the BST film post-annealed in vacuum is most likely related to the fact that the composition of the film is very close to stoichiometric one (cf. Table 3); however, further work is needed to understand this issue.

Table 3
EDX composition analysis for as-grown BST films, deposited at room temperature, and following annealing under Ar environment or vacuum. Room-temperature carrier concentrations for films annealed under Ar environment.

Sample	Bi (at%)	Sb (at%)	Te (at%)	Carrier concentration at 300 K (cm^{-3})
As deposited	11.19	28.56	60.25	–
5 h annealing in Ar	11.89	28.81	59.30	2.36×10^{19}
As deposited	11.57	28.47	59.96	–
10 h annealing in Ar	12.08	28.68	59.24	1.93×10^{19}
As deposited	10.39	28.71	60.90	–
16 h annealing in Ar	10.64	29.62	59.74	4.05×10^{19}
As deposited	8.92	29.60	61.48	–
16 h annealing in vacuum	9.71	29.09	61.20	–

Please cite this article in press as: E. Symeou, et al., Thermoelectric properties of $Bi_{0.5}Sb_{1.5}Te_3$ thin films grown by pulsed laser deposition, Appl. Surf. Sci. (2014), http://dx.doi.org/10.1016/j.apsusc.2014.10.038

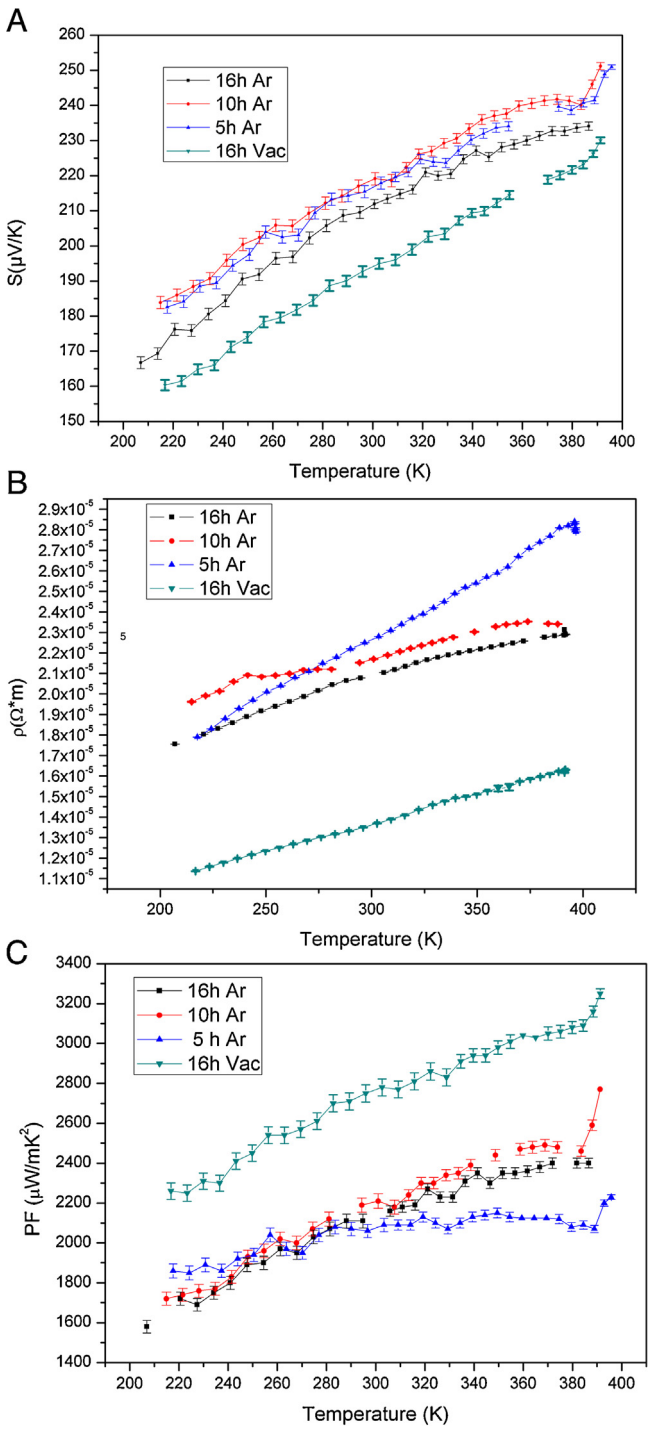

Fig. 5. Temperature dependence of electrical and thermoelectric properties of BST films grown at room temperature and post-annealed for various times at 300 °C: (a) Seebeck coefficient, (b) electrical resistivity, and (c) power factor.

4. Conclusions

In conclusion, the crystallinity and the texturing of the as-grown BST thin films increases with increasing substrate temperature. Thin films deposited at 350 °C are preferentially *c*-axis oriented. On the other hand, amorphous films deposited at room temperature upon post-annealing at 300 °C in Ar atmosphere or vacuum become polycrystalline. Both deposition and annealing of BST films at high temperatures results in an increase of antisite defects. The carrier concentration and the mobility of the BST films are enhanced with increasing substrate temperature or post-annealing treatment duration. Thermoelectric properties of room-temperature deposited BST films are significantly improved by a post-annealing treatment in vacuum at 300 °C for 16 h. The best obtained power factor at 300 K is equal to 2780 $\mu W/K^2 m$, which is among the highest ones reported for BST films grown on fused silica substrates.

Acknowledgments

This work was co-funded by the European Regional Development Fund and the Republic of Cyprus through the Research Promotion Foundation (Project ANAVATHMISI/0609/06).

References

[1] D.M. Rowe (Ed.), CRC Handbook on Thermoelectrics, CRC Press, New York, 1995.
[2] T. Caillat, M. Carle, P. Pierrat, H. Scherrer, S. Scherrer, Thermoelectric properties of $(Bi_xSb_{1-x})_2Te_3$ single crystal solid solutions grown by the T.H.M. method, J. Phys. Chem. Solids 53 (1992) 1121–1129.
[3] H. Kitagawa, A. Kurata, H. Araki, S. Morito, E. Tanabe, Structure and carrier transport properties of hot-press deformed $Bi_{0.5}Sb_{1.5}Te_3$, Phys. Status Solidi A 207 (2010) 401–406.
[4] X. Duan, J. Yang, W. Zhu, X.A. Fan, S.Q. Bao, Thickness and temperature dependence of electrical resistivity of p-type Bi0.5Sb1.5Te3 thin films prepared by flash evaporation method, J. Phys. D: Appl. Phys. 39 (2006) 5064–5068.
[5] S.J. Jeon, H. Jeon, S. Na, S.D. Kang, H.K. Lyeo, S. Hyun, H.J. Lee, Microstructure evolution of sputtered BiSb-Te thermoelectric films during post-annealing and its effects on the thermoelectric properties, J. Alloys Compd. 553 (2013) 343–349.
[6] H. Lin, K. Kang, J. Hwang, H. Ghu, H. Huang, M. Wang, Effect of annealing temperature on the thermoelectric properties of the $Bi_{0.5}Sb_{1.5}Te_3$ thin films prepared by radio-frequency sputtering, Metall. Mater. Trans. A 44 (2013) 2339–2345.
[7] D. Bourgault, C. Giroud Garampon, N. Caillault, L. Cardone, J.A. Aymami, Thermoelectric properties of n-type $Bi_2Te_{2.7}Se_{0.3}$ and p-type $Bi_{0.5}Sb_{1.5}Te_3$ thin films deposited by direct current magnetron sputtering, Thin Solid Films 516 (2008) 8579–8583.
[8] L. Cao, Y. Wang, Y. Deng, H. Gao, B. Luo, W. Zhu, Facile synthesis of preferential $Bi_{0.5}Sb_{1.5}Te_{3.0}$ nanolayered thin films with high power factor by the controllable layer thickness, J. Nanopart. Res. 15 (2013) 1.
[9] R.S. Makala, K. Jagannadham, B.C. Sales, Pulsed laser deposition of Bi_2Te_3-based thermoelectric thin films, J. Appl. Phys. 94 (2003) 3907–3918.
[10] A.A. Aziz, M. Elsayed, H.A. Bakr, J. El-Rifai, T. Van der donck, J. Celis, V. Leonov, P. Fiorini, S. Sedky, Pulsed laser deposition of bismuth telluride thin films for microelectromechanical systems thermoelectric energy harvesters, J. Electron. Mater. 39 (2010) 1920–1925.
[11] J. Schou, Physical aspects of the pulsed laser deposition technique: the stoichiometric transfer of material from target to film, Appl. Surf. Sci. 255 (2009) 5191–5198.
[12] H. Kitagawa, T. Takino, T. Tsukutani, T. Kato, M. Nanba, K. Kamata, Thermoelectric properties of $Bi_{0.5}Sb_{1.5}Te_3$ prepared by liquid-phase growth using a sliding boat, J. Electron. Mater. 42 (2013) 2043–2047.
[13] N. Peranio, M. Wnkler, M. Durrschnabel, J. Konig, O. Eibl, Assessing antisite defect and impurity concentrations in Bi_2Te_3 based thin films by high-accuracy chemical analysis, Adv. Funct. Mater. 23 (2013) 4969–4976.
[14] D. Bourgault, B. Schaechner, C.G. Garampon, T. Crozes, N. Caillault, L. Carbone, Transport properties of thermoelectric $Bi_{0.5}Sb_{1.5}Te_3$ and Bi_2 $Te_{2.7}Se_{0.3}$, J. Alloys Compd. 598 (2014) 79–84.
[15] C.N. Liao, T.H. She, Preparation of bismuth telluride thin films through interfacial reaction, Thin Solid Films 515 (2007) 8059–8060.